Numerical Investigation of Venting Through Roof for an ISO Containers

Vendra C. Madhav Rao and Jennifer X. Wen
Warwick FIRE, School of Engineering, University of Warwick
Coventry, CV4 7AL, UK

1 Abstract

Hydrogen as energy carrier is a potential alternative for reducing the greenhouse gas emissions associated with usage of hydrocarbon fuels. The ISO containers are being considered in hydrogen energy emerging technologies for housing process equipment like the standalone portable power generation unit using fuel cells. The safety concerns associated with any accidental release of hydrogen in container applications are crucial for overall design and operations of these hydrogen installations. In the present study, turbulent deflagration in premixed hydrogen-air cloud enclosed in a 20-foot container of 20’ x 8’ x 8’.6” are investigated numerically. Numerical simulations have been performed using HyFOAM, a dedicated solver developed in-house for vented hydrogen deflagration processes within the framework of the opensource computational fluid dynamics (CFD) code OpenFOAM toolbox. The flame area wrinkling combustion model is used for modelling turbulent deflagrations. Additional sub-models have been added to account for lean combustion of hydrogen-air mixtures. The numerical predictions are performed for venting through roof scenario. The predicted overpressures for venting through roof are also validated against the available recent experiments carried out by Gexcon as part of the HySEA project supported by the Fuel Cells and Hydrogen 2 Joint Undertaking (FCH 2 JU) under the Horizon 2020 Framework Programme for Research and Innovation. The numerical simulations are performed to establish the modelling approach. To further aid in filling the experimental knowledge gaps, the effect of concentration variations within the container on the generated overpressures trends are investigated.

2 Numerical modelling

The flow governing Navier-Stokes equations are solved in explicit Large Eddy Simulation (LES) method with collocated finite volume mesh approach [1]. The pressure velocity coupling is solved in Pressure-Implicit Split Operator (PISO) method. The closure for the subgrid viscosity is computed through a transport equation for subgrid kinetic energy [2]. The advective terms are discretized in second-order accurate limited-linear scheme and the temporal term are discretized using a fully implicit, second-order accurate three-time-

Correspondence to: jennifer.wen@warwick.ac.uk

level method [1]. The turbulent deflagrations are modelled using flame surface wrinkling model proposed by Weller et al. [3,4] in the LES context. The model assumes that combustion takes place in the flamelet regime in the relatively thin layers that separate regions of unburned and fully burned gases. The flame front locally propagates at unstretched laminar flame speed and under turbulence gets stretched and strained. This flame stretching due to turbulence increases flame surface area, results in an increase of the burning rate. The turbulent flame speed correlation and unstretched laminar flame speed correlation are important input parameters for this model. The volume fraction of the unburnt zone is denoted as regress variable (b), taking values of b=1 in fresh gases and b=0 in fully burnt gas region. The thermophysical process of flame propagation is represented by the transport equation for the resolved part of regress variable , given as:

$$\frac{\partial \bar{\rho}\tilde{b}}{\partial t} + \nabla.\left(\bar{\rho}\widetilde{U}\tilde{b}\right) - \nabla.\left(\bar{\rho}\mu_{sgs}\nabla\tilde{b}\right) = -\bar{\rho}_u S_L \Xi\left|\nabla\tilde{b}\right| \tag{1}$$

where, Ξ is subgrid flame wrinkling, which can be regarded as the turbulent to laminar flame speed ratio and is formally related to the flame surface density by $\sum = \Xi\left|\nabla\bar{b}\right|$, ρ is the density, S_L is laminar flame speed and μ_{sgs} is the subgrid turbulent diffusion coefficient. Symbols overbar ($\bar{}$) and tilde ($\tilde{}$) represents the filtered and the density weighted filtering operations respectively. The subscripts $'u'$ indicates conditioning on the unburned gases region. The resolved unburned gas volume fraction $\bar{b}$ is related to $\tilde{b}$ through $\bar{\rho}_u\bar{b} = \bar{\rho}\tilde{b}$. The closure for the sub-grid wrinkling is provided by a balanced transport equation,

$$\frac{\partial \bar{\rho}\Xi_t}{\partial} + \widehat{U}_s\nabla\Xi_t = \bar{\rho}G\Xi_t - \bar{\rho}R(\Xi - 1) + \bar{\rho}max[(\sigma_s - \sigma_t), 0]\Xi_t \tag{2}$$

where, $\widehat{U}_s$ is the surface filtered local instantaneous velocity of the flame, which is modelled as

$$\widehat{U}_s = \widetilde{U} + \left(\frac{\bar{\rho}_u}{\bar{\rho}} - 1\right) S_L \Xi n_f - \frac{\nabla(\bar{\rho}\mu_{sgs}\nabla\tilde{b})}{\bar{\rho}|\nabla\tilde{b}|} n_f \tag{3}$$

The direction of flame propagation is $n_f = \nabla\tilde{b}/\left|\nabla\tilde{b}\right|$, σ_s and σ_t are the surface filtered resolved strain-rates relating to the surface filtered local instantaneous velocity of the flame ($\widehat{U}_s$), modelled as

$$\sigma_t = \nabla\left(\widetilde{U} + S_L\Xi_t n_f\right) - n_f\left[\nabla\left(\widetilde{U} + S_L\Xi_t n_f\right)\right]n_f$$

$$\sigma_s = \frac{\nabla\widetilde{U} - n_f(\nabla\widetilde{U})n_f}{\Xi_t} + \frac{(\Xi_t+1)\left[\nabla(S_L n_f) - n_f[\nabla(S_L n_f)n_f]\right]}{2\Xi_t} \tag{4}$$

The terms $G\Xi_t$ and $R(\Xi_t - 1)$ in Eq. 2 are sub-grid turbulence generation and removal rate, with G and R as rate coefficients requiring modelling,

$$G = R\frac{\Xi_{eq}-1}{\Xi_{eq}} \text{ and } = \frac{0.28}{\tau_\eta}\frac{\Xi^*_{eq}}{\Xi^*_{eq}-1},$$

$$\Xi^*_{eq} = 1 + \frac{0.46}{Le}Re_t^{0.25}\left(\frac{\hat{u}}{S_{Lo}}\right)^{0.3} \text{and } \Xi_{eq} = 1 + 2(1-b)(\Xi^*_{eq} - 1) \tag{5}$$

where, τ_n is the Kolmogorov time scale, $\hat{u}$ is the sub grid turbulence intensity and Re_t is the turbulent Reynolds number. The Lewis number effects have been found to be important in numerical modelling of lean hydrogen-air combustion processes previously by many authors [5,6]. The flame wrinkling increases with decreasing Lewis number, the broadening of the flame brush happens with decreasing Lewis number. The Darrieus–Landau and thermodiffusive instabilities also affect the flame propagation in lean mixtures. Turbulent flame speed increases with decreasing Lewis number of the deficient reactant, this effect is profound for lean hydrogen mixtures, which are typical for vented explosion applications. Suitable Lewis number (Le) modelling is hence required. This is accounted for in calculating the terms in Eq.5 by taking

into account the Lewis number (Le) effects in the turbulent flame speed correlation using the algebraic reaction rate closure, MFSD of Muppala et al. [7]. The MFSD model has been successfully applied to both pure and mixed fuels, under varying Lewis number conditions [2,5-6] in both RANS and LES contexts. The predicted S_T trends are consistent with the measurements. The flame wrinkling due to the Darreius-landau instabilities is modelled as algebraic expression based on Bauwens et al. [8] as,

$$\Xi_{DL} = max\left[1, \alpha_1 \left(\frac{\Delta}{\lambda_c}\right)^{1/3}\right] \tag{6}$$

Where, λ_c is cut-off wavelength of unstable scales and $\propto_1$ is a coefficient to account for uncertainty in λ_1. The values of 7 mm and 1.3 are used for λ_c and $\propto_1$ in the current simulations to match the initial flame propagations [8]. The unstrained laminar flame speed (S_{L0}) for lean hydrogen-air mixture is adopted based on numerical study carried out by Verhelst [9], for evaluating S_L at a given equivalence ratio ($\phi = 1/\lambda$) and reference condition, expressed as power law function of elevated temperature and pressure,

$$S_L = S_{L0}(\lambda, P)\left(\frac{T_u}{T_{u0}}\right)^{\propto(\lambda,P)} \tag{7}$$

$$S_{L0} = 499.63 - 308.60\lambda + 48.887\lambda^2 - 76.238P + 4.825P^2 + 45.813\lambda P - 2.926\lambda P^2 - 7.163\lambda^2 P + 0.436\lambda^2 P^2$$

$$\alpha(\lambda, P) = 1.85175 - 0.70875\lambda + 0.50171\lambda^2 - 0.19366P + 0.0067834P^2 + 0.27495\lambda P - 0.0088924\lambda P^2 - 0.052058\lambda^2 P + 0.00146015\lambda^2 P^2$$

where S_L in cm/s , P is pressure in bar and T_u unburnt gas temperature in K. The above correlation is valid for the equivalence ratios (ϕ) between 0.33 and 0.47 (lean mixtures), pressures range of 1bar ≤ P ≤ 8.5 bar and temperature range of 300 K ≤ T ≤ 800 K, with reference state Tu_0 = 300 K. The flame wrinkling factor is eq. 1 is given as

$$\Xi = \Xi_t * \Xi_{DL} \tag{8}$$

3 Numerical setup

The computational domain is typical 20-ft ISO container of dimensions 20'x 8'x 8'.6" used in the experiments, shown in Figure 1. The walls of the container are corrugated and 2 mm in thickness. The dimensions of the container inside are 5.867 m × 2.385 m × 2.352 m. The individual vent opening area are 1 m^2 each. These vent openings are covered by either commercial vent panels or by the polyethylene sheet during the experiments. The homogeneous hydrogen-air mixture at required equivalence ratio is prepared in the container through recirculation method. Complete details about the experiments can be found in [10].

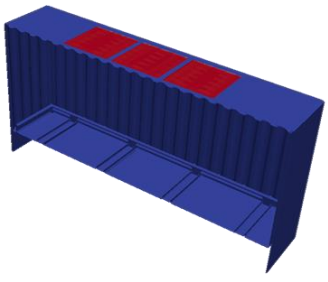

(a) Before vents are open (red - vent covered)

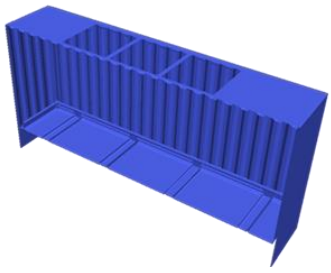

(b) After vents are open

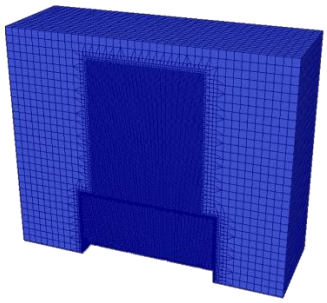

(c) Mesh distribution

Figure 1. Computational domain for six vents at roof geometry for a 20ft ISO container

The numerical simulations for venting through roof are carried out by considering two computational domains as shown in figure 1(a) and 1(b). Field values for each flow variables are mapped from domain 1(a) to domain 1(b), once the requisite vent opening overpressure is obtained during the deflagration process at any of the vent location. The requisite vent opening pressure for vent panels is set as the sum of the vent static pressure plus a delay pressure allowing of the time taken to fully open the vent. The commercial vent panels used in the experiments had a vent static pressure of 0.1 bar. The requisite vent opening pressure was then set to 0.15 bar in the numerical simulations for roof vent panels. Only half section of the container geometry is considered for simulations, taking advantage of the container's symmetry along its length. The computational domain is discretized into dominantly hexagonal finite volume mesh, with cell size varying between 3 to 6 mm in the regions of flame propagation and in remaining region cells vary between 6 mm to 50 cm (fig 1(c)). The experimental probe location are shown in figure 2.

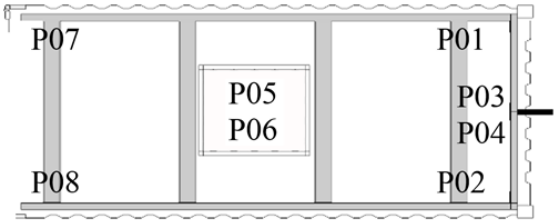

Figure 2. Internal pressure probe (P01-P08) location within the container

The probe location P01, P02, P03, P04, P07 and P08 are mounted on the U-section frame at 85mm from the side wall and 200 mm above the container floor at respective locations as shown in figure 2. The pressure probes P05 and P06 are mounted on the container roof near the vent opening. During the container roof venting experiments at Gexcon, extra clamps were used to secure the container roof attachments, which restricted the free oscillations of the container walls hence the fluid structure interactions due to the container side wall oscillations are neglected in the numerical modelling. The ignition location was at the center of the container floor. The ignition was initiated as a hot patch with product composition.

4 Results and conclusion

The numerical prediction for deflagration overpressures for 21% hydrogen concentration are plotted along with experiments in figure 3. The match between the experiments and numerical predictions are very satisfactory, peak values lie within the experimental uncertainties. The mesh refinement at the ignition location and tuning of the ignition parameters such as the ignition patch volume, ignition burnt mass fraction and ignition lag resulted in better prediction of the first overpressure peak, once these parameters are

established, they are not altered for the remaining simulations. Clearly there are two discernable pressure peak, first peak is generated when bulk of the mixture is central region of the container burns and the second peak is generated when the flame propagates to remaining mixture in the corner regions of the containers. The large negative pressure predicted in the numerical simulation are due to treating the container wall as rigid. In the Gexcon experimental campaign, only at one concentration (i.e. at 21% H_2) empty container experiment was done. It will be of interest to know the overpressure trends with change in H_2 lean concentration. Figure 4, shows the numerical prediction of peak overpressure for different H_2 concentration with in the empty container. The plots are for peak overpressure trace curves for 15%, 18% and 24% H_2-air homogenous mixture concentrations.

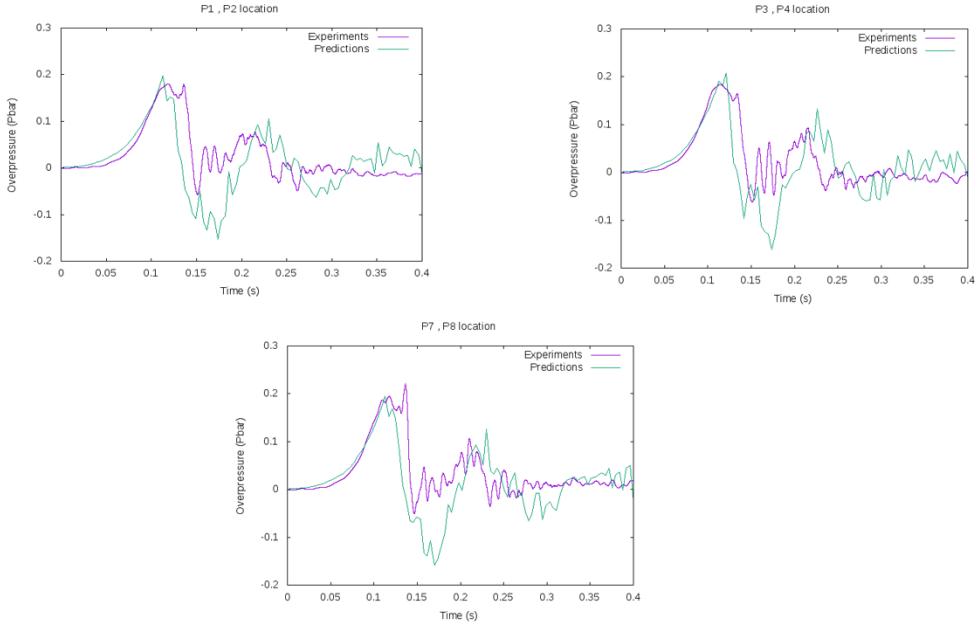

Figure 3. Overpressure plots along with experiment values for 21% hydrogen-air mixture.

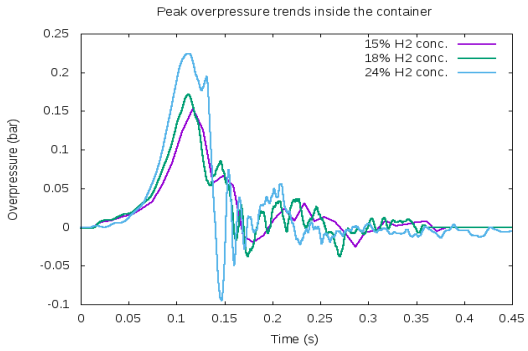

Figure 4. Peak overpressure variation for different concentration hydrogen-air mixture.

The modification to flame speed correlation and turbulent flame speed and flame instabilities considered in the present study result in reasonable accuracy of numerical predictions to experiments. Figure 4, the vented deflagrations overpressure for different % vol. concentration of hydrogen in the empty container are shown,

which are indicative of possible overpressure magnitudes that can be generated in case of any accidental hydrogen deflagration in containers. Such information is very vital in designing the vents in the process equipment and also defining the safety distances around the hydrogen process installations. The investigation of overpressure trends with model congestion within the container will be presented in a follow up publication.

Acknowledgements

The HySEA project (www.hysea.eu) receives funding from the Fuel Cells and Hydrogen Joint Undertaking under grant agreement No 671461. This Joint Undertaking receives support from the European Union's Horizon 2020 research and innovation programme and United Kingdom, Italy, Belgium and Norway.

References

[1] www.openfoam.org.

[2] Fureby, C., et al., A comparative study of subgrid scale models in homogeneous isotropic turbulence. Physics of Fluids, 1997. **9**(5): p. 1416-1429.

[3] Weller, H. G., Tabor, G., Gosman, A. D., and Fureby, C., Application of a flame wrinkling LES combustion model to a turbulent mixing layer (1998), Proc. of Combust. Inst., 27.

[4] Tabor, G. and H.G. Weller, Large Eddy Simulation of Premixed Turbulent Combustion Using Ξ Flame Surface Wrinkling Model. Flow, Turbulence and Combustion, 2004. 72(1): p. 1-27.

[5] Abdel-Gayed R. G., Bradley, D, Hamid M., N. Lawes, M., Lewis number effects on turbulent burning velocity (1985), Twentieth Sym. on Combust.

[6] Chakarborty, N., Cant, R.S, Effects of Lewis number on flame surface density transport in turbulent premixed combustion (2011). Comb. and Flame. 9:158.

[7] Bauwens, C.R., Chaffee, J., and Dorofeev, S.B., "Experimental and Numerical Study of Hydrogen-Air Deflagrations in a Vented Enclosure," in 7th ISHPMIE proceedings Vol. 1, St. Petersburg, Russia, 2008.

[8] Muppala Reddy, S. P., Aluri Naresh K., Dinkelacker, F., Development of an algebraic reaction rate closure for the numerical calculation of turbulent premixed methane, ethylene, and propane/air flames for pressure up to 1.0 MPa (2005), Combust. And Flame, 140.

[9] Verhelst, S., A laminar velocity correlation for hydrogen/air mixtures at spark ignition engine conditions (2003), Spring Technical Conf. of ASME internal Combust. Engine division, ICE2003.

[10] Skjold, Trygve, Hisken, Helene, Lakshmipathy, Sunil, Atanga, Gordon, van Wingerden, Matthijs, Olsen, Kjetil Lien, Holme Morten Norlemann, Turoy, Nils Martin, Mykleby, Martin, Kess,(2017) "Vented hydrogen deflagrations in containers : Effect of congestion for homogenous mixtures". Zenodo. http://doi.org/10.5281/zenodo.998039.